Modeling of avalanche photodiodes by Crosslight APSYS

Y. G. Xiao*, Z. Q. Li, Z. M. Simon Li
Crosslight Software Inc., 206-3993 Henning Dr., Burnaby, BC V5C 6P7 Canada

ABSTRACT

Avalanche photodiodes (APDs) are being widely utilized in various application fields where a compact technology computer aided design (TCAD) kit capable for APD modeling is highly demanded. In this work, based on the advanced drift and diffusion model with commercial software, the Crosslight APSYS, avalanche photodiodes, especially the InP/InGaAs separate absorption, grading, charge and multiplication (SAGCM) APDs for high bit-rate operation have been modeled. Basic physical quantities like band diagram, optical absorption and generation are calculated. Performance characteristics such as dark- and photo-current, photoresponsivity/multiplication gain, breakdown voltage, excess noise, frequency response and bandwidth etc., are simulated. The modeling results are selectively presented, analyzed, and some of results are compared with the experimental. Device design optimization issues are further discussed with respect to the applicable features of the Crosslight APSYS within the framework of drift-diffusion theory.

Keywords: Avalanche multiplication, InP/InGaAs SAGCM APD, avalanche photodiodes, photodetectors, opto-electronic devices, semiconductor device modeling, modeling software, optic fiber communication

1. INTRODUCTION

Avalanche photodiodes (APDs) have found extensive applications in various fields such as particle detection, confocal microscopy, astronomical observation, optical range finding, ultrasensitive fluorescence and optic fiber receiver modules etc. As a front-end photodetector for the high sensitive optic receiver, InP/InGaAs APD plays an important role for modern long haul and high bit-rate optical fiber communication systems. In today's commercial market, the 2.5 and 10 giga-bit/s optical receiver modules based on InP/InGaAs APDs have demonstrated superior performance characteristics. The practical InP/InGaAs APD based on the separate absorption, grading, charge and multiplication (SAGCM)[1-3] structure is of particular importance with demonstrated performance such as high internal gain, improved reliability[4,5] and high gain-bandwidth product in excess of 100 GHz[6]. In recent years, this basic SAGCM structure has been coupled with the resonant cavity[7-10] to achieve improved performance such as low multiplication noise, high quantum efficiency, maximum unity-gain bandwidth and record-high gain-bandwidth product of 290 GHz[7,8]. Waveguide APDs incorporating SA(G)CM structure have also been developed recently[11,12].

Despite of the significant amount of experimental efforts for the development of photodetectors, better modeling techniques, especially compact technology computer aided design (TCAD) kits capable to simulate photodetectors including APDs are highly demanded. This is particularly indispensable for APDs because of their internal gain mechanism with impact ionization. The stochastic characteristic of the impact ionization makes it difficult to extract detailed design information for APDs simply by experimental trials and measurement data inspection. The routine request to consider several tradeoff issues simultaneously among all the performance characteristics, as the matter of fact, makes the design optimization process for APDs probably one of the most time and cost consuming. Good TCAD kit with improved modeling techniques would enable saving the overall time and cost in comparison with the attempts based solely on experimental fabrication. It will also help to analyze the performance characteristics, optimize device design and predict the operation characteristics. Academically, modeling approaches based on the stochastic or statistic approaches have been explored to study the time domain/frequency responses during the evolution of APD history[13-22]. Modeling techniques based on drift-diffusion model[23,24] to study DC characteristics have also been explored. However, these approaches emphasize more on the specific aspects of APDs with simple device structures. Comprehensive modeling for all the performance characteristics and for the advanced complex photodetectors is not always available. For example, the drift-diffusion modeling gave good 2D simulation on the device physical quantities and DC performance characteristics such as carrier concentration, dark- and photo-current etc, the important bandwidth characteristics is, however, not seen in the publications by using such a drift-diffusion approach.

*yxiao@crosslight.com; phone: 1-604-320-1704; fax: 1-604-320-1734; www.crosslight.com

Infrared and Photoelectronic Imagers and Detector Devices II, edited by Randolph E. Longshore, Ashok Sood,
Proc. of SPIE Vol. 6294, 62940Z, (2006) · 0277-786X/06/$15 · doi: 10.1117/12.681189

Crosslight has developed a dynamic numerical approach for impulse response modeling in the time domain based on the drift-diffusion model. This enables modeling of nearly all the aspects of the performance characteristics for APDs. In this work, based on Crosslight's device simulator, the APSYS, simulation has been performed for InP/InGaAs SAGCM APDs. This paper is organized as follows. In section 2, the simulator APSYS and basic theoretic background are briefly described. The device structure and simulation details are explained in section 3. Modeling results, analyses and discussion are presented in section 4. Finally, a summary is given in section 5.

2. SIMULATOR APSYS AND THEORETIC BACKGROUND

The simulator APSYS is a general-purpose 2D/3D finite element analysis and modeling software for semiconductor devices. It includes many advanced physical models and offers a flexible modeling and simulation environment. Advanced features include heterojunction models, (quantum) tunneling, hot carrier transport, trap dynamics, impact ionization and non-isothermal analysis etc. The simulator solves several interwoven equations including the basic Poisson's equation, and drift-diffusion current equations for electrons and holes. Poisson's equation is as follows[25],

$$-\nabla\cdot\left(\frac{\varepsilon_0\varepsilon_{dc}}{q}\nabla V\right)=-n+p+N_D(1-f_D)-N_A f_A+\sum_j N_{tj}\left(\delta_j-f_{tj}\right) \tag{1}$$

and here the last term describes the deep trap density effect. In the above equation, V is electrical potential, ε_0 vacuum dielectric constant, ε_{dc} relative DC or low frequency dielectric constant, q electronic charge, n electron concentration, p hole concentration, N_D the shallow donor density, N_A the shallow acceptor density, f_D occupancy of the donor level, f_A occupancy of the acceptor level, N_{tj} the density of the jth deep trap, f_{tj} the occupancy of the jth deep trap level, and δ_j is 1 for donor-like traps and 0 for acceptor-like traps. The current continuity equations for electrons and holes are respectively expressed as

$$\nabla\cdot J_n-\sum_j R_n^{tj}-R_{sp}-R_{st}-R_{au}+G_{opt}(t)=\frac{\partial n}{\partial t}+N_D\frac{\partial f_D}{\partial t}, \tag{2}$$

$$\nabla\cdot J_p+\sum_j R_p^{tj}+R_{sp}+R_{st}+R_{au}-G_{opt}(t)=-\frac{\partial p}{\partial t}+N_A\frac{\partial f_A}{\partial t}. \tag{3}$$

Here J_n and J_p are electron and hole current flux density respectively. R_n^{tj} and R_p^{tj} are electron and hole recombination rates per unit volume through the jth deep trap respectively. G_{opt} is the optic generation rate, R_{sp}, R_{st}, and R_{au} the spontaneous recombination rate, the stimulated recombination rate and the Auger recombination rate per unit volume respectively. These equations govern the electrical behavior (e.g., I-V characteristics) of a semiconductor device.

The carrier mobilities μ_n and μ_p account for the scattering mechanism for electrical transport. The software simulator provides several mobility model options, from constant values to field dependant ones. A commonly used mobility model has the following form for electrons and holes respectively.

$$\mu_n=\frac{\mu_{0n}}{\left[1+\left(\mu_{0n}F/v_{sn}\right)^{\beta_n}\right]^{1/\beta_n}}\qquad\qquad \mu_p=\frac{\mu_{0p}}{\left[1+\left(\mu_{0p}F/v_{sp}\right)^{\beta_p}\right]^{1/\beta_p}} \tag{4}$$

Here F is the electric field, v_{sn} and v_{sp} the saturation velocity for electron and hole, μ_{0n} and μ_{0p} the low field electron and hole mobilities, and β_n and β_p constant values corresponding to electron and hole respectively. Many III-V compound semiconductors (e.g., GaAs) exhibit negative differential resistance due to the transition of carriers into band valleys with lower mobility. The simulator has implemented the following field dependant mobility model for electrons in this case,

$$\mu_n=\frac{\mu_{0n}+\left(v_{sn}/F_{0n}\right)\left(F/F_{0n}\right)^3}{1+\left(F/F_{0n}\right)^4} \tag{5}$$

where F_{0n} is the threshold electric field for the field dependent mobility. The simulator also provides an option to include the impurity dependence of the low field mobility.

To describe impact ionization, Crosslight has implemented both the Baraff's model[26] and Chynoweth's empirical formula[27]. A generalized Chynoweth's formula has the following format[28],

$$\alpha,\beta=A_c\exp\left[-\left(F_c/F\right)^{\kappa_n}\right]. \tag{6}$$

Here A_c, F_c and κ_n are a set of three empirical parameters, which can be different for electrons and holes. The electron and hole have the same expression, and usually the impact ionization coefficient for electron is expressed as α and for hole as β. Crosslight has also implemented the carrier energy balance equation for hydrodynamic modeling. A generation rate G for the impact ionization is implemented as follows[28],

$$G = (\alpha J_n + \beta J_p)/q \tag{7}$$

The excess noise factor F can be evaluated by using the McIntyre's expression[29] as follows.

$$F = M\left\{1-(1-k_{eff})\left(\frac{M-1}{M}\right)^2\right\} \tag{8}$$

Here k_{eff}=α/β because it is a pure hole injection case for the investigated SAGCM APD structure described below.

3. DEVICE STRUCTURE AND SIMULATION DETAILS

The basic InP/InGaAs SAGCM APD structure[22,30-32] is schematically shown in Fig. 1 (a). Only the central active region is of interest for investigation in this work. As seen from the figure, the n$^-$ $In_{0.53}Ga_{0.47}As$ absorption layer is near the bottom substrate. The n InGaAsP grading, n$^+$ InP charge and n$^-$ InP multiplication layers are grown subsequently. The important feature for this structure is that the multiplication region is separated from the absorption region so that the avalanche multiplication occurs mostly in a wider bandgap InP layer while the absorption occurs in a narrower bandgap InGaAs layer. The n$^+$ InP charge sheet layer can help to maintain high electric field across the whole multiplication region and reduced electric field for the absorption region. The n InGaAsP grading layer can help to overcome the possible hole trapping problem at the heterointerface. When reverse-biased, holes will be injected into the multiplication layer to initiate impact ionization. The photon illumination (1.55 μm) is from the top front.

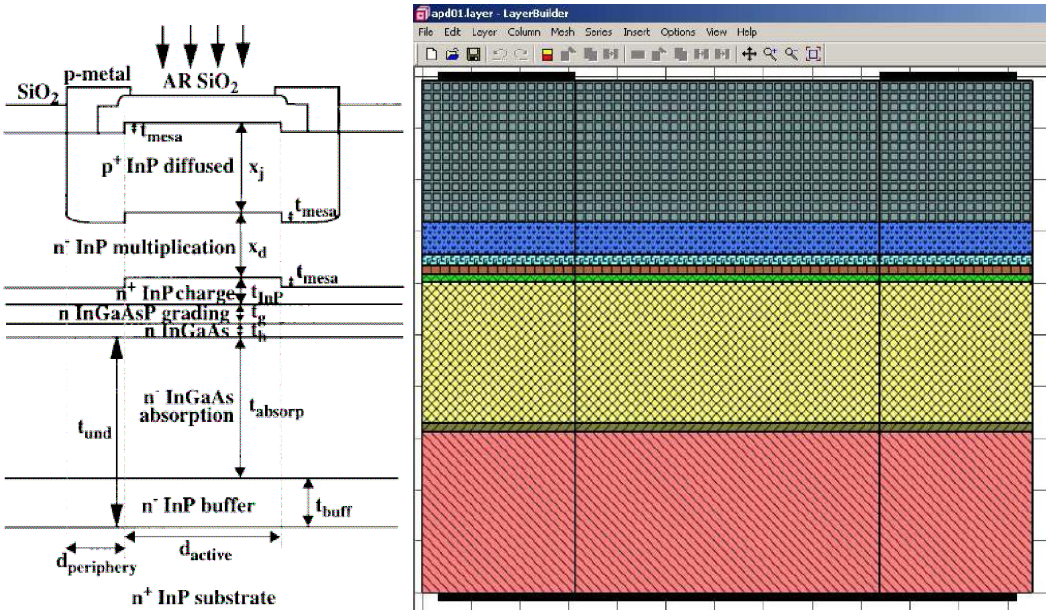

(a) (b)

Fig. 1. (a) Schematic InP/InGaAs SAGCM APD structure, and (b) schematic layer view generated by Crosslight APSYS simulator.

With a friendly-using LayerBuilder provided by Crosslight APSYS, a three-column device structure has been built up for the investigated APD structure (see Fig. 1 (b)). The top contact pads are put on the top of the 1st and 3rd columns, and a top window for the 2nd (middle) column is left for front illumination. For one-dimensional simulation, here we have ignored the difference between the lateral periphery region and the central active region. We have also replaced the thin n$^-$ InP buffer layer with a graded InGaAsP layer for the convenience of modeling. The so-built layer structure forms a 2D cross section, and the schematic layer view for the investigated SAGCM APD is displayed in Fig. 1 (b). The thickness and dopant density for each epitaxy growth layer is displayed in Table 1 below.

Table 1. Thicknesses, dopant densities for the epitaxy layers, and other major parameters used for the simulation. Thickness *t* and *x* are in μm, and dopant density is in 10^{22} m^{-3}.

t_{sub}	2.5	N_{sub}	1000
t_{buff}	0.1	N_{buff}	0.005
t_{absorp}	1	N_{absorp}	0.0338
t_h	0.02	N_h	0.0675
t_q	0.09	N_q	0.0675
t_{InP}	0.17	N_{InP}	10
x_d	0.3	N_d	0.0675
x_j	2.2	N_j	500
$E_{g\text{-}InP}$	1.347 eV	$E_{g\text{-}InGaAs}$	0.75 eV
C	0.2 pF	R	50 Ω

From the layer file, the simulator can generate files for mesh, material and doping information, which will be subsequently cited by the solving file for simulating the device. In the solving file, the Chynoweth's empirical model is used to turn on the impact ionization. Although the effect from front antireflection (AR) coating and back side reflection could also be simulated by adding corresponding command lines in the solving file of APSYS, it has been ignored in this work. The DC performance characteristics like dark-current, photo-current and breakdown, together with some physical properties such as bandgap, electric field profile, impact ionization coefficients etc., could be quickly obtained. From the photo-current, one could easily obtain the breakdown voltage. The multiplication gain could also be extracted from the photo-current IV curve by scaling the photo-current with one at the unity gain where the impact ionization is just initiated. From the computed electric field profile and the impact ionization coefficients, one could calculate the excess noise factor according to McIntyre's expression (see Eq. (8)). Since the electric field across the multiplication region is almost flat at high biases, this usually gives a feasible way to evaluate the excess noise factor. In order to evaluate the –3 dB bandwidth, time domain impulse response modeling has to be performed. This involves in turning on the illumination for a short period of time and then turning off the illumination for further relaxation of a long period of time under a specific bias (corresponding to a specific gain value). The time domain impulse response data is further fast Fourier transformed (FFT) into the frequency response data, from which the –3 dB bandwidth is evaluated. A load circuit effect (load resistance and capacitance product, *RC*, see Table 1) is also added when calculating the –3 dB bandwidth.

4. RESULTS, ANALYSES AND DISCUSSION

The simulation results can be at first examined with the band diagram. The equilibrium band diagram is displayed in Fig. 2 (a), where we could see how the band gap varies as growth layers go from substrate (0-2.5 μm distance region) to the top Zn diffused p^+ InP region. One could also notice the bandgap change across the grading layer between InP and InGaAs region.

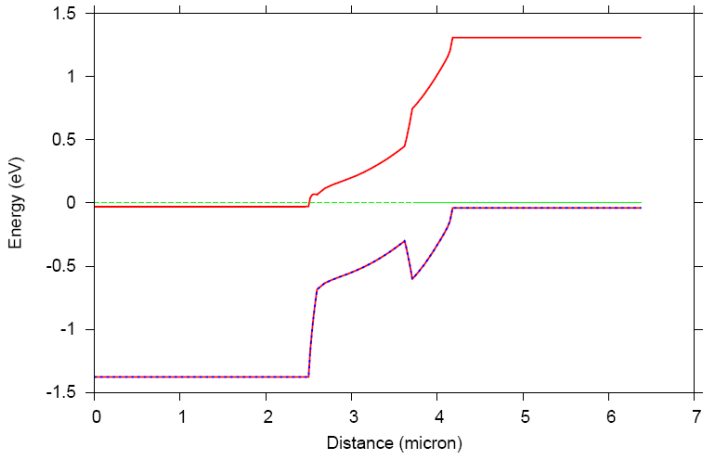

Fig. 2. Equilibrium band diagram of the InP/InGaAs SAGCM APD. The distance origin starts from the n^+ InP substrate.

The 2D relative energy density profile is also displayed in Fig. 3 (a), where the 1.55-μm photon illumination is mainly absorbed by the narrow bandgap InGaAs layer. This is also reflected in the profile of optical generation rate, which is presented in Fig. 3 (b). The photon-generated electron-hole pairs are mainly from the absorption region and they will drift under electric field toward their corresponding contact terminals for current collection. The holes, however, have to experience impact ionizations in the multiplication region during the course traveling to the top p^+ InP layer. The electric field profile is displayed in Fig. 4 (a), where the electric field is high across the multiplication region. This leads to the significant impact ionization rate in this region as seen in Fig. 4 (b).

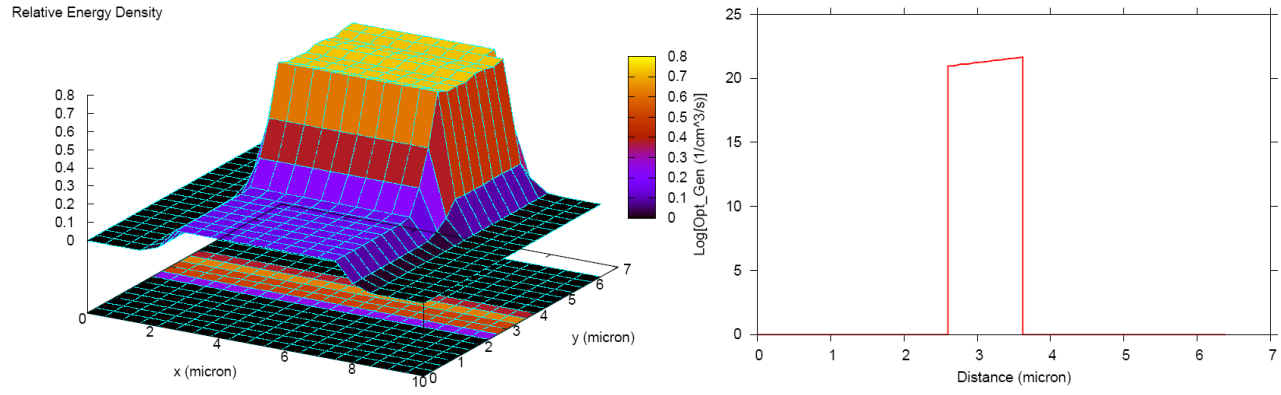

(a) (b)

Fig. 3. (a) 2D relative energy density profile, and (b) optical generation rate for the InP/InGaAs SAGCM APD investigated.

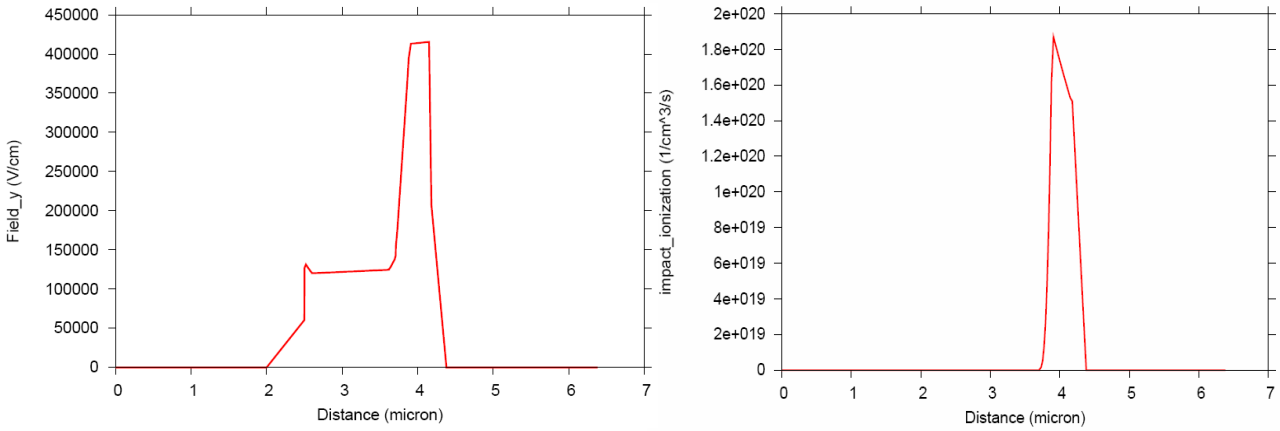

(a) (b)

Fig. 4. (a) Electric field profile, and (b) impact ionization rate for the InP/InGaAs SAGCM APD investigated.

The simulated dark- and photo-current IV curves are presented in Fig. 5 (a), and it shows a breakdown voltage about 30.45 V. The bias for unity gain is at about 10.15V. The extracted multiplication gain is presented in Fig. 5 (b), which is in good agreement with the experimental results[22]. The excess noise factor calculated from McIntyre's expression is displayed in Fig. 6, and more accurate computation of this characteristic relies on the calibration of the electron and hole impact ionization coefficients for InP in the high electric field range investigated.

Bandwidth is an important characteristic of APDs for application in optic fiber communication. The time domain impulse responses simulated by Crosslight APSYS are presented in Fig. 7 (a) at various reverse biases (correspondingly various multiplication gain). As seen in the figure, it generally takes long time to achieve the peak response and long relaxation time back to the dark background at large reverse biases. This corresponds to the so-called gain-bandwidth limit for large reverse bias or large multiplication gain region. The –3 dB bandwidths as extracted from the FFT frequency responses are presented in Fig. 7 (b), where the modeling results are also compared with the experimental. Good agreement between the experimental and the modeling is observed. The obtained gain-bandwidth product is estimated to be about 60 GHz.

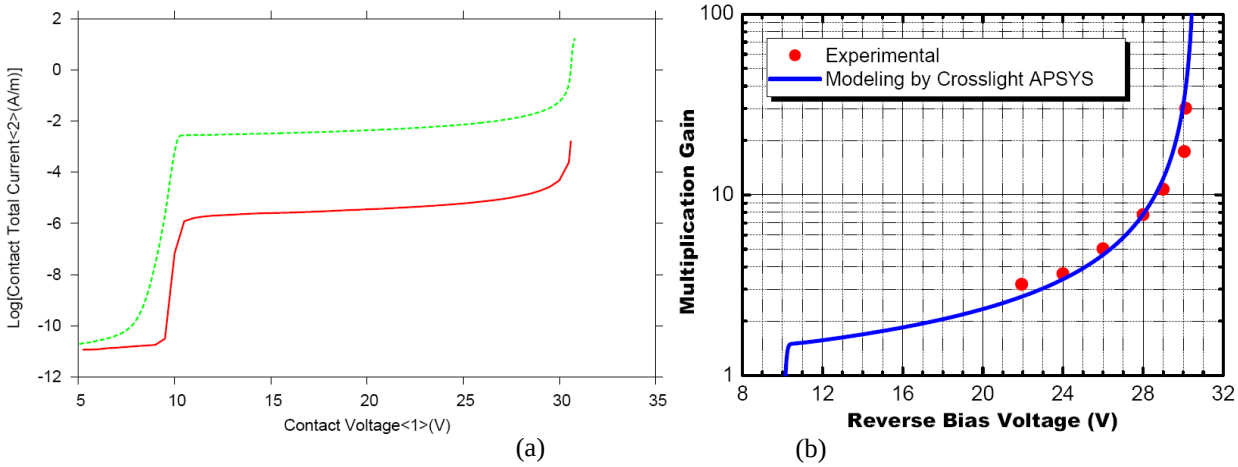

Fig. 5. (a) Dark- (lower curve) and photo-current (upper curve) IV characteristics, and (b) comparison of the simulated multiplication gain with the experimental for the InP/InGaAs SAGCM APD investigated.

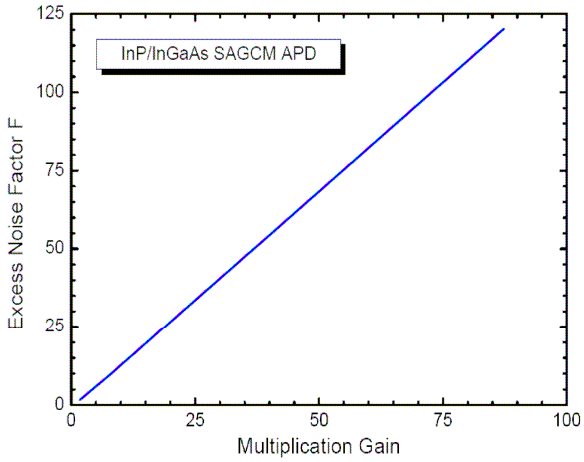

Fig. 6. Simulation results of excess noise factor vs multiplication gain for the investigated SAGCM APD.

For the simulated device itself, it seems that it is not optimized for the 10 giga-bit/s optical fiber communication system. It is believed that the bandwidth in the top bandwidth ceiling region (gain from 2 or 3 to 12 or 15 with the bandwidth-vs-gain curve) should be at least 7.1 GHz[30]. The InP/InGaAs APD feasible for 10 giga-bit/s operation is predicted to be with a multiplication layer thickness less than 0.3 μm[30]. The dead space effect is important for APDs with thin multiplication layer. Crosslight has implemented an energy-balanced hot carrier model to approach this issue. Initial simulation indicates that the hot carrier model could give a more appropriate simulation for the dark- and photo-current. The influence on the impulse responses and bandwidth characteristics are currently under investigation and implementation.

Besides the bandwidth characteristics, APDs are usually troubled by the premature edge breakdown, which affects the reliable and stable operation. A 2D simulation is usually needed to address this issue[31,32]. Crosslight APSYS provides powerful 2D capability to model complicated device structure shape, like diffused guard rings, and the relevant results will be reported elsewhere.

Another important issue for APDs is to maintain a certain responsivity value for a normal operational condition. For example, an unity-gain responsivity of 0.7 A/W is usually the design bottom line. This issue is complicated with the bandwidth requirement. Techniques like microlenses have been developed to improve the responsivity, but novel device structure can usually give better design solution to circumvent this tradeoff problem. Resonant-cavity (RC) APDs have been demonstrated with high bandwidth and high responsivity[7-10]. Crosslight APSYS is also capable to simulate such resonant cavity enhanced devices (like RC LED[33]), and the relevant modeling work for RC APD is currently under way.

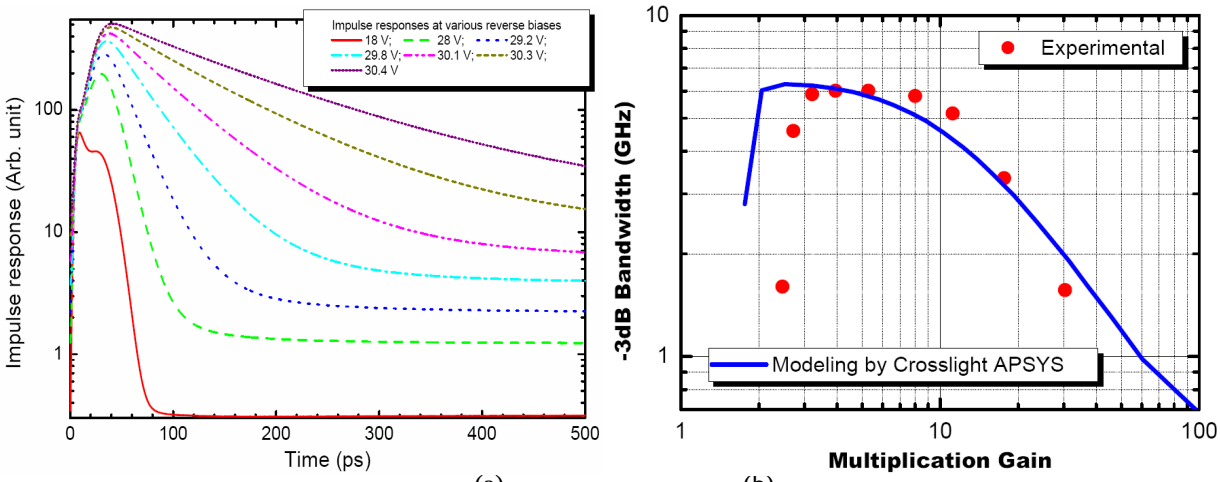

(a) (b)

Fig. 7. (a) Impulse responses at various reverse biases, and (b) the –3 dB bandwidth vs multiplication gain for the investigated InP/InGaAs SAGCM APD.

5. SUMMARY

In summary, based on the advanced drift and diffusion model and commercial software, the Crosslight APSYS, avalanche photodiode, especially the InP/InGaAs SAGCM APDs for multi-giga-bit operation have been modeled. Basic physical quantities like band diagram, optical absorption and generation are calculated. Performance characteristics such as dark- and photo-current, photoresponsivity/multiplication gain, breakdown voltage, excess noise, frequency response and bandwidth etc., are simulated. The modeling results are selectively presented, analyzed, and some of results are compared with the experimental. Device design optimization issues are further discussed with respect to the applicable features of the Crosslight APSYS within the framework of drift-diffusion theory. The demonstrated results together with various capable features make Crosslight APSYS a powerful TCAD kit to simulate the photosensitive and other advanced semiconductor devices.

ACKNOWLEDGMENTS

This work is supported by the IR&D Fellowship from the Natural Sciences and Engineering Research Council of Canada.

REFERENCES

1. L. E. Tarof, D. G. Knight, T. Baird, and K. E. Fox, C. J. Miner, N. Puetz, and H. B. Kim, “Planar InP/InGaAs avalanche photodetectors with partial charge sheet in dvice periphery,” *Appl. Phys. Lett.* 57, pp. 670-672 (1990).
2. P. P. Webb, R. J. McIntyre, J. Scheibling, and M. Holunga, “Planar InGaAs/InP APD fabrication using vapor-phase epitaxy and silicon implantation techniques,” in *Optical Fiber Communications Conf.*, Technical Digest Series Vol. 1, pp. 129-131 (1988).
3. R. Kuchibhotla, and J. C. Campbell, “Delta-doped avalanche photodiodes for high bit-rate lightwave receivers,” *J. Lightwave Technol*. 9, pp. 900-905 (1991).
4. S. An, M. J. Deen, A. S. Vetter, W. R. Clark, J. -P. Noel, and F. R. Shepherd, “Effect of mesa overgrowth on low-frequency noise in planar separate absorption, grading, charge, and multiplication avalanche photodiodes,” *IEEE J. Quantum Electron.* 35, pp. 1196-1202 (1999).
5. S. An, M. J. Deen, “Low-frequency noise in single growth planar separate absorption, grading, charge, and multiplication avalanche photodiodes,” *IEEE Trans. Electron. Dev.* 47, pp. 537-543 (2000).
6. L. E. Tarof, “Planar InP/InGaAs avalanche photodetector with a gain-bandwidth product in excess of 100 GHz,” *Electron. Lett*. 27, pp. 34-36 (1991).
7. H. Nie, O. Baklenov, P. Yuan, C. Lenox, B. G. Streetman, and J. C. Campbell, “Quantum-dot resonant-cavity separate absorption, charge, and multiplication avalanche photodiode operating at 1.06 μm,” *IEEE Photon. Technol. Lett.* 10, pp. 1009-1011 (1998).

8. C. Lenox, H. Nie, P. Yuan, G. Kinsey, A. L. Homles, Jr., B. G. Streetman, and J. C. Campbell, "Resonant-cavity InGaAs-InAlAs avalanche photodiodes with gain-bandwidth product of 290 GHz," *IEEE Photon. Technol. Lett*. 11, pp. 1162-1164 (1999).
9. Y. G. Xiao and M. J. Deen, "Theoretical approach to frequency response of resonant cavity avalanche photodiodes," *Proc. SPIE* 4288, pp. 21-30 (2001).
10. Y. G. Xiao and M. J. Deen, "Frequency response and modeling of resonant-cavity separate absorption, charge and multiplication avalanche photodiodes," *J. Lightwave Technol*. 19, pp. 1010-1022 (2001).
11. G. S. Kinsey, J. C. Campbell, and A. G. Dentai, "Waveguide avalanche photodiode operating at 1.55 μm with a gain-bandwidth product of 320 GHz," *IEEE Photon. Technol. Lett*. 13, pp. 842-844 (2001).
12. J. Wei, F. N. Xia, and S. R. Forrest, "A high-responsivity high-bandwidth asymmetric twin-waveguide coupled InGaAs-InP-InAlAs avalanche photodiode," *IEEE Photon. Technol. Lett*. 14, pp. 1590-1592 (2002).
13. J. C. Campbell, B. C. Johnson, G. J. Qua and, W. T. Tsang, "Frequency response of InP/InGaAsP/InGaAs avalanche photodiodes," *J. Lightwave Technol*. 7, pp. 778-784 (1989).
14. R. B. Emmons, "Avalanche-photodiode frequency response," *J. Appl. Phys*. 38, pp. 3705-3714 (1967).
15. G. Kahraman, B. E. A. Saleh, W. L. Sargeant, and M. C. Teich, "Time and frequency response of avalanche photodiodes with arbitrary structure," *IEEE Trans. Electron. Dev*. 39, pp. 553-560 (1992).
16. T. Shiba, E. Ishimura, K. Takahashi, H. Namizaki, and W. Susaki, "New approach to the frequency response analysis of an InGaAs avalanche photodiode," *J. Lightwave Technol*. 6, pp. 1502-1506 (1988).
17. J. N. Hollenhorst, "Frequency response theory for multilayer photodiodes," *J. Lightwave Technol*. 8, pp. 531-537 (1990).
18. J. C. Campbell, W. S. Holden, G. J. Qua, and A. G. Dentai, "Frequency response of InP/InGaAsP/InGaAs avalanche photodiodes with separate absorption 'grading' and multiplication regions," *IEEE J. Quantum Electron*. 21, pp. 1743-1746 (1985).
19. W. S. Wu, A. R. Hawkins, and J. E. Bowers, "Frequency response of avalanche photodetectors with separate absorption and multiplication layers," *J. Lightwave Technol*. 14, pp. 2778-2785 (1996).
20. M. M. Hayat and B. E. A. Saleh, "Statistical properties of the impulse response function of double-carrier multiplication avalanche photodiodes including the effect of dead space," *J. Lightwave Technol*. 10, pp. 1415-1425 (1992).
21. M. M. Hayat, B. E. A. Saleh, and M. C. Teich, "Effect of dead space on gain and noise of double-carrier-multiplication avalanche photodiodes," *IEEE Trans. Electron. Dev*. 39, pp. 546-552 (1992).
22. A. Bandyopadhyay, M. J. Deen, L. E. Tarof, and W. Clark, "A simplified approach to time domain modeling of avalanche photodiodes," *IEEE J. Quantum Electron.* 34, pp. 691-699 (1998).
23. J. W. Parks, A. W. Smith, K. F. Brennan, and L. E. Tarof, "Theoretical study of device sensitivity and gain saturation of separate absorption, grading, charge, and multiplication InP/InGaAs avalanche photodiodes," *IEEE Trans. Electron. Dev*. 43(12), pp. 2113-2121 (1996).
24. J. N. Haralson II, J. W. Parks, K. F. Brennan, W. Clark, and L. E. Tarof, "Numerical simulation of avalanche breakdown within InP-InGaAs SAGCM standoff avalanche photodiodes," *J. Lightwave Technol*. 15(11), pp. 2137-2140 (1997).
25. Crosslight technical manuals, Copyright © Crosslight Software Inc. (2005).
26. G. A. Baraff, "Distribution function and ionization rates for hot electrons in semiconductors," *Phys. Rev*. 128, pp. 2507-2517 (1962).
27. A. G. Chynoweth, "Ionization rates for electrons and holes in Silicon," *Phys. Rev*. 109, pp. 1537-1540 (1958).
28. S. Selberherr, "Analysis and simulation of semiconductor devices," Copyright © Springer-Verlag, Wien-New York (1984).
29. R. J. McIntyre, "Multiplication noise in uniform avalanche diodes," *IEEE Trans. Electron. Dev.* 13, pp. 164-158 (1966).
30. Y. G. Xiao, I. Bhat, and M. N. Abedin, "Performance dependences on multiplication layer thickness for InP/InGaAs avalanche photodiodes based on time domain modeling," *Proc. SPIE* 5881, pp. 196-205 (2005).
31. Y. G. Xiao and M. J. Deen, "Modeling of two-dimensional gain profiles for InP/InGaAs avalanche photodiodes with a stochastic approach," *IEEE J. Quantum Electron.* 35(12), pp. 1853-1862 (1999).
32. Y. G. Xiao and M. J. Deen, "Two-dimensional gain profiles of InP/InGaAs separate absorption, grading, charge and multiplication avalanche photodiodes modeled by a simplified stochastic approach," *J. Vac. Sci. Technol. A* 18(2), pp. 610-614 (2000).
33. Crosslight technical presentations, http://crosslight.com/downloads/downloads.html